First-passage-time processes and subordinated Schramm-Loewner evolution

M. Ghasemi Nezhadhaghighi,[1] M. A. Rajabpour,[2] and S. Rouhani[1]
[1]*Department of Physics, Sharif University of Technology, Tehran, P.O. Box 11365-9161, Iran*
[2]*SISSA and INFN, Sezione di Trieste, via Bonomea 265, 34136 Trieste, Italy*
(Received 14 February 2011; revised manuscript received 17 April 2011; published 25 July 2011)

We study the first-passage-time processes of the anomalous diffusion on the self-similar curves in two dimensions. The scaling properties of the mean-square displacement and mean first passage time of the fractional Brownian motion and subordinated walk on the different fractal curves (loop-erased random walk, harmonic explorer, and percolation front) are derived. We also define natural parametrized subordinated Schramm-Loewner evolution (NS-SLE) as a mathematical tool that can model diffusion on fractal curves. The scaling properties of the mean-square displacement and mean first passage time for NS-SLE are obtained by numerical means.

DOI: 10.1103/PhysRevE.84.011134 PACS number(s): 02.50.−r, 61.41.+e, 05.30.Pr

I. INTRODUCTION

The anomalous or non-Fickian diffusive transports have attracted a lot of interest in the past few years. There is a wide range of heterogeneous or pre-asymptotic systems in the fields of physics, astronomy, biology, chemistry, and economics, where anomalous diffusion occurs [1]. This phenomenon is observed in diffusion on fractal structures in geophysical and geological media [2,3], charge transport in disordered and amorphous semiconductors [4], acceleration of particles inside a turbulent medium [5], transport process in the biological systems [6], and many other examples; for an extensive collection of references see [1]. The well-known examples of anomalous diffusion are the continuous-time random walk (subdiffusive processes) [7] and Lévy flight [8]. In this type of process, the mean-square displacement (MSD) obeys a power law equation with respect to time with exponent $0 < \nu < 2$. Anomalous transport, especially the continuous-time random walk and Lévy flight, can be studied within the fractional Fokker-Planck (FP) equation approach [9].

One of the most important characteristics in normal and anomalous diffusions is first passage time (FPT), which is defined as the time needed for the dynamic variable to cross a given threshold value for the first time [10,11]. FPT has been used to characterize diffusive processes in various systems such as the spreading of disease [12], the passage of polymers and DNA in subdiffusive media and membranes [13], the firing of neurons [14], animals searching for food [15], and Lévy stable random motion [8].

One of the interesting aspects of the diffusion problem is the study of FPT processes in fractal geometries such as percolating fronts, crack patterns, polymer chains, lightning paths, etc. [16–20]. In this work we are interested in simple fractal objects with fractal dimension $1 < d_f < 2$ without any branch point. Since the coordination number of all the points on the fractal is 2, it is easy to conclude that there should be lots of similarities between FPT processes in these systems and one-dimensional (1D) systems. This was already discussed in Ref. [21], and the important rule of the length of the fractal objects in FPT processes was understood. In Ref. [21] the connection with the Schramm-Loewner evolution (SLE) [22] was also discussed; the important rule of the definition of the length in the SLE studies [21,23] was especially emphasized. In this paper we will generalize the work done in Ref. [21], in many different directions. To have an idea of fractal objects with fractal dimension $1 < d_f < 2$ we will study the scaling exponents of MSD and mean FPT (MFPT) of the diffusing particles on loop-erased random walk (LERW), harmonic explorer (HE), and percolation fronts (PF's) on the upper half-plane. We will study different random walkers such as fractional Brownian motion and subordinated walk on the fractal curves. The scaling properties of the MSD of the walker and MFPT will be discussed. Finally we present a method to study diffusion on fractal curves by using the SLE. We show that all the scaling behaviors discussed for the discrete fractal curves can be rederived by using the subordinated natural SLE, which is the time-changed Schramm-Loewner evolution. The central aim of this work is to use the subordinated natural SLE to find a new connection between diffusion on the self-similar traces and the SLE as a growth process. Our analyses of MSD and MFPT are the key points of this connection. The paper is organized as follows: In Sec. II we will fix the notation and introduce the scaling relations for the diffusion problem on semi-1D fractal paths, where we measure the scaling exponents of MSD and MFPT for two-sided diffusion and diffusion with waiting times on the self-similar curves with fractal dimension d_f. In Sec. III we use the Schramm-Loewner evolution as a mathematical model to introduce new classes of diffusion processes (subordinated SLE). The results of this section are compatible with the two-sided diffusion and diffusion with waiting time on the discrete fractal paths. In Sec. IV we conclude our findings. To be self-explanatory, we add three appendices explaining the details of our simulation methods.

II. FIRST PASSAGE TIME IN LATTICE FRACTAL INTERFACES

We begin by considering the diffusion problem on semi-1D random curves. For our purposes we restrict ourselves to the fractal curves with Hausdorff dimensions $1 < d_f < 2$ [16] that start from the origin and remain in the upper half-plane. To understand statistical properties of diffusion along such inhomogeneous paths it is important to first introduce the diffusion problem in the 1D case.

A. First-passage-time statistics in the one-dimensional domain

Consider a one-dimensional diffusion X_t with dynamics

$$dX_t = a(X_t)dt + \sigma dW_t, \tag{1}$$

where W_t is a one-dimensional stochastic process. The interval for the solution of Eq. (1) is defined as closed on the left-hand side $x_a = 0$ and open on the right-hand side $x_b = R$. These special choices force the diffusing particle to move only in $x \geqslant 0$.

An interesting problem in the theory of stochastic processes is finding the time that a particle takes to reach a certain level. The problem of finding this time is called first passage time [10,11]. The first passage time is the time τ_r taken for the process, having started from $x = 0$, to be reached in $x = r$ [11]:

$$\tau_r = \inf\{t > 0 | X_t = r\}, \tag{2}$$

where the infimum for every subset S of real numbers is denoted by $\inf\{S\}$ and defined to be the biggest real number that is smaller than or equal to every number in S.

Clearly FPT is a random variable that varies from one sample of X_t to another. In general we are interested in those processes where the two statistical variables $\langle X_t^2 \rangle$ and $\langle \tau_r \rangle$ have scaling behavior,

$$\langle X_t^2 \rangle \propto t^{\nu}, \quad \langle \tau_r \rangle \propto r^{\beta}. \tag{3}$$

One example of Eq. (1) is $a = 0$, $\sigma = 1$, and $W_t = |B_t^H|$, where B_t^H is the fractional Brownian motion (fBm) process. Note that fBm with Hurst index $0 < H < 1$ is the only self-similar Gaussian process with stationary increments [24]. The correlation function of fBm is

$$\langle B^H(t) B^H(s) \rangle \sim [|t|^{2H} + |s|^{2H} - |t - s|^{2H}]. \tag{4}$$

The absolute value of B_t^H is used to force the diffusing particle to move only in the region $x \geqslant 0$. The particle's position $X_t = |B_t^H|$ is a stochastic variable with

$$\langle X_t^2 \rangle = \langle |B_t^H|^2 \rangle \sim t^{2H}. \tag{5}$$

The scaling relation in Eq. (5) is in agreement with Eq. (3) and shows that $\nu = 2H$ [25]. Diffusion is said to be anomalous if $\nu \neq 1$, where $0 < \nu < 1$ ($1 < \nu < 2$) indicates the subdiffusive (superdiffusive) behavior.

It is easy to determine the exponent $\beta = 1/H$ analytically for the mentioned boundary condition. To find the scaling parameter β, consider a random process X_t as $X_{t/\lambda^{1/H}} = \frac{1}{\lambda} X_t$. Now one can replace $r \to \lambda r$ in Eq. (2) to find $\tau_{\lambda r}$. It is straightforward to show that $\tau_{\lambda r}$ is the same as $\lambda^{1/H} \tau_r$ in the distributional sense. By this scaling argument, one can observe that MFPT is given by

$$\langle \tau_r \rangle \propto r^{1/H}. \tag{6}$$

It is worth mentioning that by choosing $W_t = |B_t|$, where B_t is a Brownian motion (fBm with $H = \frac{1}{2}$), one can use the Fokker-Planck equation, which describes the space-time evolution of the probability density function (PDF) of X_t, to find FPT distribution. More details can be found in [26].

Although studying diffusion in one-dimensional systems is interesting for its own sake, there are many examples of diffusion in self-similar interfaces with fractal dimensions $1 < d_f < 2$. We will generalize the above arguments to self-similar interfaces with arbitrary fractal dimension, and we will study the statistical properties of the diffusion on the fractal curves.

To motivate our method of measurement of the scaling parameters ν, β for diffusing particle on the fractal curves, we first consider models on a lattice domain, e.g., the loop-erased random walk, harmonic explorer, and percolation explorer processes.

1. The loop-erased random walk

The LERW on the square lattice domain is a random walk with erased loops when they appear. This process is stopped when it reaches a given length. To produce LERW curves started from the origin and conditioned to be in the upper half-plane, one can use the reflecting boundary condition on the real axis for the random walker. The fractal dimension of LERW is 5/4 [27].

2. Explorer processes

Explorer processes (EP's) on honeycomb lattice, such as the percolation front process with $d_f = \frac{7}{4}$ and the harmonic explorer process with $d_f = \frac{3}{2}$, are used as other classes of fractal interface [28,29]. To construct an EP path with a fixed number of steps N, we used a process from a class of explorer processes on the honeycomb lattice. This process is called the overruled harmonic explorer process [30]. For numerical analysis, we simulated this process on the extremely large rectangular domain, where it can approximate the upper half-plane (see Appendix A).

Although other studies such as [21] have also used self-similar traces to study the FPT problem, they have not characterized the scaling relations in measurable quantities such as the MSD and MFPT for the general diffusion processes, e.g., two-sided diffusion and diffusion with the waiting time, which we have studied in our simulations.

B. Two-sided diffusion on the fractal paths

In this subsection we study the statistical properties of the diffusing particles along self-similar curves. An interesting problem in this direction is the determination of the scaling exponents of the random displacement.

For a one-dimensional domain with reflecting boundary condition, we mentioned in Sec. II A that the MSD and the MFPT, according to Eqs. (5) and (6), respectively, obey scaling laws with the exponents $\nu = 2H$ and $\beta = 1/H$. In the following we explain how to use the discrete random walk model to simulate the stochastic process X_t on the 1D domain with reflecting boundary condition on $x = 0$, and we then favorably apply this model to the random process on the discrete fractal curves.

First we consider the random walker on the one-dimensional discrete lattice. This random walker started from the position $x = 0$ at $t_0 = 0$ and at time $t_n = n\delta t$ moves one step to the right (left) when $\{|B_{t+\delta t}^H| - |B_t^H|\} > 0$ ($\{|B_{t+\delta t}^H| - |B_t^H|\} < 0$). The normal random walk (discrete version of Brownian motion) corresponds to $H = 1/2$. This random process corresponds to two-sided diffusion on the 1D domain.

Following the idea presented in one dimension, we obtain the statistics of two-sided diffusion on the fractal curves. To this aim we consider a random walker with position coordinates X_n and Y_n for the nth walk where $(X_0,Y_0) = (0,0)$ is the start position and it moves back and forth along the discrete self-similar curve. In order to simulate a random walker on the curve that started from the origin and remains in the upper half-plane, we used, from the fBm process, $|B_t^H|$. Using this correlated stochastic process we define another stochastic process S_n^H so that $S_{n+1}^H = S_n^H + 1$ ($S_{n+1}^H = S_n^H - 1$) when $\{|B_{t+\delta t}^H| - |B_t^H|\} > 0$ ($\{|B_{t+\delta t}^H| - |B_t^H|\} < 0$) with the initial value $S_0^H = 0$. The random walk position can be defined by $X_n = x(S_n^H)$ and $Y_n = y(S_n^H)$ where $x(i)$ and $y(i)$ are the position components of the ith point of the curve.

We now study numerically the scaling dependence of $\langle R_n^2\rangle = \langle X_n^2 + Y_n^2\rangle$ and $\langle \tau_r\rangle$ to n and r for many random walkers moving along such self-similar one-dimensional objects. In particular, we study the scaling forms of $\langle R_n^2\rangle$ and $\langle \tau_r\rangle$.

To study the scaling laws in two-sided diffusion, it should be mentioned here that the scaling exponents $\nu(H,d_f)$ and $\beta(H,d_f)$ in two-sided diffusion on the fractal curves are in general a function of the Hurst parameter H and geometrical dimension d_f. Within the FPT statistics of the one-dimensional diffusing particle approach, one can consider the self-similar curve as a one-dimensional nonstraight line with length l. For this semi-1D object using Eq. (6) one can observe that $\langle \tau_l\rangle \propto l^{1/H}$. On the other hand, for a fractal curve (with length l) inside a circle there is a scaling law $l \propto r^{d_f}$ where r is the radius of the circle. Under these assumptions, the MFPT reads as $\langle \tau_r\rangle \propto r^{d_f/H}$.

The very same method can be applied to the scaling law of MSD. In the same manner as before we consider the fractal curve a semi-1D object. There is a scaling relation $\langle l_n^2\rangle \propto n^{2H}$ [similar to Eq. (5)] for the position of the diffusing particle l_n after n walks along such a semi-1D curve. In addition, the scaling relation $l_n \sim R_n^{d_f}$ for the fractal curve is well-known, where R_n is the radius of the semicircle-enclosed l_nth walks. We therefore obtain a universal law $\langle R_n^2\rangle \propto n^{2H/d_f}$ for MSD of two-sided diffusing particles on the fractal curves. Using these arguments we expect

$$\nu(H,d_f) = 2H/d_f, \quad \beta(H,d_f) = d_f/H. \tag{7}$$

These equations are in agreement with the scaling exponents in Eqs. (5) and (6) in the $d_f \to 1$ limit. The above results for $H = \frac{1}{2}$ recover the predictions in Ref. [21]. Table I summarizes our numerical results for the two scaling exponents ν and β, where it can be seen that our results are quite compatible with the predictions in Eq. (7) for two-sided diffusion on the fractal curves. In our measurements we used from 50 000 fractal curves and 10 independent realizations of random process S_n^H per curve for each numerical test.

C. Diffusion with waiting times on the fractal curves

In this subsection we study anomalous motion of a free particle with waiting time on the self-similar curve. In the preceding section, we obtained statistics of walkers moving back and forth randomly along self-similar discrete curves. The physical time between two consecutive steps of walks in the previous examples is equal to a constant Δt.

We can also consider the random time elapsing between two consecutive jumps of a diffusing particle. The particle starts from the origin and is trapped in site n for some random time. These positive random waiting times τ_n are identically distributed random variables, each having the same probability density function $\psi(\tau)$ [3,7]. The role of the waiting time forces us to identify operational time $S_{t_n}^\alpha = \sum_n \tau_n$ and physical time $t_n = n\Delta t$. The physical time n is always accelerated against the strictly increasing random time $S_{t_n}^\alpha$. The random time $S_{t_n}^\alpha$ is called subordinator. As mentioned in Refs. [31–33] it is described as

$$S_{t_n}^\alpha = \inf\{\tau_m : U(\tau_m) > t_n\}, \tag{8}$$

where $U(\tau_m)$ is an α-stable subordinator ($0 < \alpha < 1$) and $\tau_m = m\Delta\tau$. The random process $S_{t_n}^\alpha$ is called the inverse-time α-stable subordinator. The above process has neither stationary nor independent increments, but it is easy to show that we have distributional scaling $S_{\lambda t}^\alpha = \lambda^\alpha S_t^\alpha$, which leads us to the following symmetry for the subordinated Brownian motion:

$$B\left(S_{ct}^\alpha\right) = B\left(c^\alpha S_t^\alpha\right) = c^{\alpha/2} B\left(S_t^\alpha\right). \tag{9}$$

Although $B(S_t^\alpha)$ is self-similar with a Hurst exponent $\alpha/2$, it is not fractional Brownian motion because it does not have a Gaussian distribution and it does not have stationary increments. The process S_t^α is strictly increasing and it tends to infinity for $t \to \infty$ so it is a good process to consider as the time, whereas in the $\alpha \to 1$ limit the subordinated time converges to the physical time. In our study we generated the subordinator $S_{t_n}^\alpha$ following Ref. [32] (see Appendix B).

We study statistical properties of position coordinates $X_n = x(S_{t_n}^\alpha)$ and $Y_n = y(S_{t_n}^\alpha)$ for a subordinated walker with operational time $S_{t_n}^\alpha$ that moves on the discrete self-similar curve with fractal dimension d_f and position components $x(i)$ and $y(i)$. For this class of particle diffusion in the fractal path, we again expect universal scaling dependence of the MSD ($\langle R_n^2\rangle = \langle X_n^2 + Y_n^2\rangle$) and the MFPT ($\langle \tau_r\rangle$) to the geometrical parameters n and r as

$$\nu(\alpha,d_f) = 2\alpha/d_f, \quad \beta(\alpha,d_f) = d_f/\alpha. \tag{10}$$

TABLE I. Numerical values of the scaling exponents ν and β for the two-sided diffusion on the fractal curves. To measure these exponents we used from correlated process S_n^H with $H = 0.8$ and 0.9.

Model	$\nu\,(H = 0.8)$	$\beta\,(H = 0.8)$	$\nu\,(H = 0.9)$	$\beta\,(H = 0.9)$
LERW	1.280 ± 0.001	1.56 ± 0.01	1.437 ± 0.005	1.385 ± 0.005
HE	1.066 ± 0.001	1.88 ± 0.01	1.195 ± 0.005	1.670 ± 0.003
PF	0.92 ± 0.01	2.17 ± 0.01	1.029 ± 0.003	1.945 ± 0.005

TABLE II. Numerical values of the scaling exponents ν and β for subordinated diffusion on the fractal curves. To measure these exponents we used from subordination $S^{\alpha}_{t_n}$ with $\alpha = 0.8$ and 0.9.

Model	$\nu\,(\alpha = 0.8)$	$\beta\,(\alpha = 0.8)$	$\nu\,(\alpha = 0.9)$	$\beta\,(\alpha = 0.9)$
LERW	1.280 ± 0.001	1.56 ± 0.01	1.440 ± 0.001	1.39 ± 0.01
HE	1.065 ± 0.005	1.88 ± 0.01	1.200 ± 0.001	1.67 ± 0.01
PF	0.920 ± 0.005	2.18 ± 0.01	1.030 ± 0.005	1.95 ± 0.01

Our numerical results for $\alpha = 0.8$ and $\alpha = 0.9$ (see Table II) are in good agreement with the scaling exponents in Eq. (10).

III. FIRST PASSAGE TIME AND SCHRAMM-LOEWNER EVOLUTION

In the preceding section we studied scaling exponents of MSD and MFPT for some important examples of two-sided and subordinated diffusion on the discrete self-similar curves in the upper half-plane. In our study we used three statistical models: loop-erased random walk, harmonic explorer, and percolation interfaces on the lattice.

The scaling limit of the lattice models as the lattice spacing goes to zero corresponds to Schramm-Loewner evolution. This mathematical model is defined in the complex plane and it was introduced by Schramm [22]. SLE is based on the Loewner equation,

$$\partial_t g_t(z) = \frac{2}{g_t(z) - \xi_t}, \tag{11}$$

where the real-valued function ξ_t is called the driving (or forcing) function, which determines all the properties of SLE. Loewner showed that for any nonintersecting curve parametrized by a complex function $\gamma(t)$ in the upper half-plane $\mathbb{H}$, there exists a conformal map $g_t(z)$, which maps the upper half-plane minus the curve and the region that is separated from infinity by the curve (hull: K_t) $\mathbb{H} \setminus K_t$ to the upper half plane $\mathbb{H}$ [34]. Ordinary SLE is the Loewner evolution with $\xi_t = \sqrt{\kappa} B_t$, where B_t is the Brownian motion with mean zero and $E[B_t B_s] = \min(t,s)$ and also with the diffusion constant $\kappa > 0$ [22]. These properties ensure that the curve is conformally invariant.

SLE_κ is a random conformally invariant curve with the fractal dimension $d_f = 1 + \kappa/8$ $(0 < \kappa < 8)$ [28,35]. The scaling limits of LERW, HE, and PF are SLE_κ with $\kappa = 2$, 4, and 6, respectively [27,36,37].

The SLE_κ curve $[\gamma(t)]$ is parametrized with time t. On the other hand the lattice models (LERW, HE, and PF) usually have a natural parametrization given by the number of steps with equal length along the curve. In general, the scaling limits of the lattice models are not the same as SLE_κ, where this difference comes from parametrization of each model [38]. We will use from an appropriate method to reparametrize the SLE_κ curve.

A. Natural parametrized SLE

The first step in simulating SLE is time-step discretization. Let us consider a partition of the time interval $[0,t]$, where it is discretized into $0 = t_0 < t_1 < t_2 < \cdots < t_n = t$. One method to simulate SLE is the foregoing approximation with the equally spaced discrete time points $t_i = idt$. In this method the points z_i on the curve $\gamma(t)$ are given by an iteration process $z_i = f_1 \circ f_2 \circ \cdots \circ f_j(\xi_j)$, where $f_j(z) = \sqrt{(z - \xi_j)^2 - 4dt} + \xi_j$ is the inverse conformal map and ξ_j is the discretized drift, where it will be approximated by a piecewise constant function in the uniform partition of the time interval $[(i-1)dt, idt]$. Notice that the conformal map $f_i(\xi_i)$ can produce a small slit at ξ_j with length $L_i = \mathrm{Im}[f_i(\xi_i)] = 2\sqrt{t_{i+1} - t_i}$ on the upper half-plane. In this method the two-dimensional distances $l_i = |\gamma(t_i) - \gamma(t_{i-1})|$ are extremely nonuniform [23,38,39].

We hereby, require the natural parametrized SLE_κ (N-SLE_κ) curve, where it is the discrete SLE_κ curve $\{\gamma_i\}$ with an approximately equal step length $|\gamma(t_i) - \gamma(t_{i-1})| \approx \lambda$. There are some mathematical and numerical procedures used to find a sensible definition of N-SLE_κ [23,39,40] (see Appendix C).

B. Subordinated SLE

In order to understand the scaling relations for the models of diffusion with waiting time on the self-similar traces as well as two-sided diffusion on the fractal curves, we present here the subordinated version of SLE_κ.

The motivation of our approach comes from the idea that the probability distribution of the point at the tip of the SLE_κ trace satisfies the Fokker-Planck equation (FPE) [41], which basically can be thought of as the FPE of the position of a particle in the fractal interface. In a similar manner one may think about the FPE for the probability distribution of the tip of the N-SLE and also the subordinated N-SLE (NS-SLE) curve in the continuum limit and study diffusion. In principle it should be possible to calculate analytically MSD and MFPT for these semi-1D interfaces by using the FPE in two dimensions. Unfortunately we do not know how to write the FPE of the N-SLE and NS-SLE; therefore we just calculate numerically the scaling properties of the tip of the NS-SLE as the diffusion process on the fractal paths. We will show that the scaling behaviors of the subordinated N-SLE are similar to the lattice models.

For normal SLE given by Eq. (11) the time variable is deterministic, but we would like to set this variable as an internal parameter τ that is also stochastic and strictly nondecreasing; this is called subordinating the process by the inverse-time α-stable subordinator S^{α}_t (see Appendix B).

Using the above definition one can consider Loewner's map with the new time as $g_{S^{\alpha}_t}(z)$, which is still scale invariant in the following sense: the conformal map $\tilde{g}_{S^{\alpha}_t}(z) = \frac{1}{\lambda^{\alpha/2}} g_{S^{\alpha}_{\lambda t}}(\lambda^{\alpha/2} z)$ with $\tilde{B}(S^{\alpha}_t) := \frac{1}{\lambda^{\alpha/2}} B(S^{\alpha}_{\lambda t})$ satisfies the same Loewner equation as $g_t(z)$. The above scale invariance enforces the scale invariance of the curve.

We discussed the simulation of SLE and N-SLE in the preceding section. The simulation of subordinated SLE (S-SLE) and natural parametrized subordinated SLE (NS-SLE) are similar. The only difference is the conformal map $f_j(z) = \sqrt{[z - \xi(S^{\alpha}_{t_j})]^2 - 4dS^{\alpha}_{t_j}} + \xi(S^{\alpha}_{t_j})$, a where $dS^{\alpha}_{t_n} = S^{\alpha}_{t_n} - S^{\alpha}_{t_{n-1}}$ and $0 = t_0 < t_1 < t_2 < \cdots < t_n = t$. The time steps $\Delta_j = dt$ $(t_i = \sum_{j=1}^{i} \Delta_j)$ in the case of S-$\mathrm{SLE}^{\alpha}_\kappa$ are selected uniformly and in the NS-$\mathrm{SLE}^{\alpha}_\kappa$ the non-uniform time

TABLE III. Numerical values of the scaling exponents ν and β for the tip of the NS-SLE$_\kappa^\alpha$ curves with $\kappa = 2.0$, 4.0, and 6.0 and $\alpha = 0.8$ and 0.9.

NS-SLE$_\kappa^\alpha$	$\nu\,(\alpha = 0.8)$	$\beta\,(\alpha = 0.8)$	$\nu\,(\alpha = 0.9)$	$\beta\,(\alpha = 0.9)$
$\kappa = 2.0$	1.28 ± 0.02	1.52 ± 0.05	1.42 ± 0.04	1.35 ± 0.05
$\kappa = 4.0$	1.02 ± 0.05	1.84 ± 0.04	1.16 ± 0.05	1.63 ± 0.05
$\kappa = 6.0$	0.92 ± 0.03	2.15 ± 0.05	1.00 ± 0.03	1.90 ± 0.06

steps Δ_i are computed by using Jacobian scheme. The only difference between S-SLE$_\kappa^\alpha$ (NS-SLE$_\kappa^\alpha$) and normal SLE$_\kappa$ (N-SLE$_\kappa$) is in the growth process of each of them. In the first case the tip of the curve has waiting time according to the α-stable Levy process.

As discussed earlier, the scaling exponents ν and β for a subordinated walk along discrete fractal interfaces are defined explicitly in Eq. (10), where they are in agreement with numerical simulations. We will consider the tip of NS-SLE$_\kappa^\alpha$ as a subordinated growth process, where it is a mathematical model for a subordinated walk along fractal curves. The scaling exponents of this subordinated process are collected in Table III, where they are in good agreement with Eq. (10) and also with the numerical simulation of the subordinated random walk along the self-similar discrete curves (see Table II).

We also notice that another way to subordinate the forcing function in Eq. (11) is based on the iterated Brownian motion [42]. Consider two stochastic processes, B_t and Y_t^H, where the first one is the Brownian motion and the second one is the fractional Brownian process. The iterated Brownian process is defined as $B(|Y_t^H|)$, where $|Y_t^H|$ corresponds to the nonnegative random time. It is easy to verify that the fractional Brownian time Brownian motion $B(|Y_t^H|)$ is a self-similar process of index $H/2$, that is, for any λ,

$$B\left(\left|Y_{\lambda t}^H\right|\right) = B\left(\lambda^H \left|Y_t^H\right|\right) = \lambda^{H/2} B\left(\left|Y_t^H\right|\right). \tag{12}$$

Simulation of the the natural parametrized version of fractional Brownian time SLE (NF-SLE$_\kappa^H$) is similar to the NS-SLE case. First consider discrete times $0 = t_0 < t_1 < t_2 < \cdots < t_n = t$ and the conformal map $f_j(z) = \sqrt{[z - \xi(|Y_{t_j}^H|)]^2 - 4d|Y_{t_j}^H|} + \xi(|Y_{t_j}^H|)$, where the infinitesimal values of the local time $d|Y_{t_j}^H| = |Y_{t_j}^H| - |Y_{t_{j-1}}^H|$ can get positive and negative values. The length of NF-SLE$_\kappa^H$ curves increases for $d|Y_{t_j}^H| > 0$ and decreases for $d|Y_{t_j}^H| < 0$. This dynamical process is very similar to the two-sided diffusion on the lattice fractal models. Our estimations for the two scaling parameters ν and β for MSD and MFPT, Table IV, are in a good agreement with the predicted values in Eq. (7) and also numerical results coming from the lattice models (see Table I).

TABLE IV. Numerical values of the scaling exponents ν and β for the tip of the NF-SLE$_\kappa^H$ curves with $\kappa = 2.0$, 4.0, and 6.0 and $H = 0.8$ and 0.9.

NF-SLE$_\kappa^H$	$\nu\,(H = 0.8)$	$\beta\,(H = 0.8)$	$\nu\,(H = 0.9)$	$\beta\,(H = 0.9)$
$\kappa = 2.0$	1.28 ± 0.01	1.57 ± 0.01	1.44 ± 0.01	1.40 ± 0.02
$\kappa = 4.0$	1.05 ± 0.03	1.90 ± 0.02	1.16 ± 0.05	1.70 ± 0.04
$\kappa = 6.0$	0.90 ± 0.03	2.20 ± 0.02	1.01 ± 0.03	2.00 ± 0.05

IV. CONCLUSIONS

To conclude, we studied the diffusive dynamics of the random processes on the self-similar curves and measured the scaling exponents of mean-squared displacement and mean first passage time expressed in Eq. (3). The various scaling exponents for MSD and MFPT are obtained numerically for two-sided diffusion and diffusion with waiting time on three discrete fractal curves, i.e., the loop-erased random walk, harmonic explorer, and percolation front. It appears that the exponents only depend on the fractal dimension d_f of the curves and the scaling exponent H for the two-sided diffusion and α for the subordinated diffusion.

Finally, we rederived the properties of the anomalous diffusion (FPT, MSD) on the discrete fractal curves with a subordinated version of the natural parametrized SLE. Our results offer a method to investigate diffusion in the fractal interfaces. We believe that these results are a starting point for the development of the subordinated version of SLE.

ACKNOWLEDGMENT

M. G. Nezhadhaghighi kindly acknowledges intensive discussions with Marco Gherardi.

APPENDIX A

To find the harmonic explorer and percolation fronts, we used the overruled harmonic explorer process on a very large rectangular domain. This domain on the upper half-plane as shown in Fig. 1 is splitting into three parts: a left boundary with yellow (light gray) condition, a right boundary with blue (dark gray), and also an uncolored inner part. This boundary condition is used to limit the EP path to this part of half-plane to start from r_0 and stop when it reaches r_* or length N. The explorer process is the unique path from the origin. In each step, there is a yellow (light gray) hexagon on the left and a blue (dark gray) one on the right [29].

To generate this path dynamically, a growth process starts from the point r_0 on the lower boundary. In the first step the color of face f_1 in front of r_0 is chosen to make it blue (dark gray) or yellow (light gray) and the explorer is forced to turn left or right, respectively. To choose the color of face f_1, a random walker starts from f_1 and stops when it crosses the rectangle's boundary for the first time. Now, the color of f_1 with probability $0 < p < 1$ is yellow (light gray) if the touch boundary is yellow (light gray). Note that two stochastic operations are used to color one hexagon: a random walker to find the boundary color and flip of a coin to accept or not accept the boundary color. The new tip of explorer path is located in the position r_1 and a new face (f_2) should be colored with the same restriction. In particular, the outcomes of the explorer process with $p = \frac{1}{2}, 1$ as shown in Fig. 2 are percolation front and harmonic explorer, respectively. The fractal dimension of the overruled harmonic explorers has a linear relationship with p and it is conjectured to be $d_f = 2 - \frac{p}{2}$ [30].

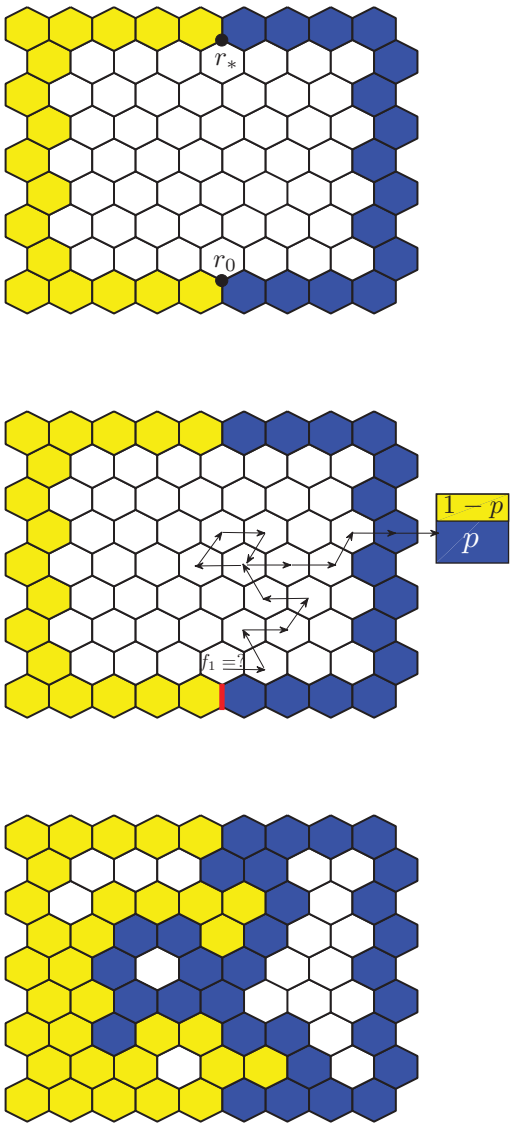

FIG. 1. (Color online) A rectangular domain with appropriate boundary conditions is used to build an explorer path. Top: Three parts of the domain, which consists of a left boundary with yellow (light gray) hexagons, a right boundary with blue (dark gray) hexagons, and uncolored hexagons. Middle: First step to identify color of face f_1. A random walker moves around uncolored sites to hit the boundary. In this example, the color of face f_1 with probability p will be blue (dark gray) or with probability $1-p$ will be yellow (light gray). Notice that the walker turns to right when yellow (light gray) is selected and turns to left when blue (dark gray) is selected. Bottom: A complete exploration process in a rectangle.

APPENDIX B

The celebrated subordinated random time S_t^α is given by Eq. (8), where it can be efficiently generated by the algorithm proposed in Ref. [32]. As mentioned earlier the α-stable subordinator $U(\tau)$ denotes the strictly increasing Levy motion with the Laplace transform $\langle e^{-kU(\tau)}\rangle = e^{-\tau k^\beta}$ [33]. The first step in simulating S_t^α begins with approximating of the strictly increasing α-stable Levy motion $U(\tau)$ on the discrete times

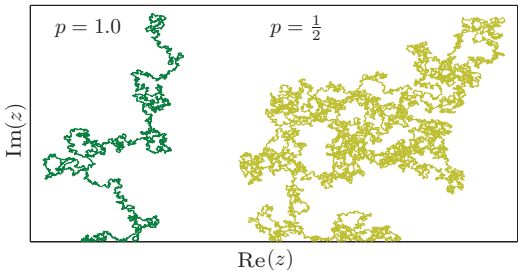

FIG. 2. (Color online) The overruled harmonic explorer path with length $N = 3 \times 10^4$. Left: harmonic explorer with $p = 1.0$ and fractal dimension $d_f = 3/2$. Right: percolation explorer with $p = 1/2$ and fractal dimension $d_f = 7/4$.

$\tau_i = i\Delta\tau$ $(i = 0,1,\ldots,M)$. The numerical integration of the process $U(\tau)$ for $0 < \alpha \leqslant 1$ yields

$$U(\tau_{j+1}) = U(\tau_j) + \Delta\tau^{1/\alpha} L_\alpha(\beta), \tag{B1}$$

where $L_\alpha(\beta)$ is a Levy stable random variable with parameter β and $U(0) = 0$. We use skewed Levy-stable distribution ($\beta = 1$) to ensure that $U(\tau)$ gets an almost increasing random process [33]. It can be generated by

$$L_\alpha(1.0) = \frac{\sin\left[\alpha\left(V + \frac{\pi}{2}\right)\right]}{[\cos(V)]^{1/\alpha}} \times \left\{\frac{\cos\left[V - \alpha\left(V + \frac{\pi}{2}\right)\right]}{W}\right\}^{(1-\alpha)/\alpha}, \tag{B2}$$

where V is a random variable with uniform distribution between $(-\frac{\pi}{2}, \frac{\pi}{2})$ and W has exponential distribution with mean 1. For the time horizon T, the summation process in Eq. (B1) ends when we get $U(\tau_{M-1}) \leqslant T < U(\tau_M)$. One can observe that $U(\tau)$ is strictly increasing and M always exists [32].

Now, for every $t_i \in (0 = t_0 < t_1 < t_2 \ldots < t_N = T)$, we find τ_j such that $U(\tau_{j-1}) < t_i \leqslant U(\tau_j)$, and from the definition in Eq. (8) we can define $S_{t_i}^\alpha = \tau_j$. From Eqs. (B1) and (B2) it is clear that $L_\alpha(1) = 1$ and $S_{t_i}^\alpha = t_i$ in the $\alpha \to 1$ limit, where at this limit subordinated time converges to the normal time.

APPENDIX C

A standard procedure [39] to find the half plane N-SLE$_\kappa$ trace is based on a change in the size of the ith slit length L_i (it is a function of time-step parameter $\Delta_i = t_i - t_{i-1}$ as $L_i = 2\sqrt{\Delta_i}$) by the Jacobian. The Jacobian $|J_{i-1}| \approx |(\xi_i - \xi_{i-1})G''_{i-1}(\xi_{i-1})|$ of the conformal map $G_i = f_1 \circ f_2 \circ \cdots \circ f_i$ acts on the corresponding segment to rescale the length L_i for the ith slit by

$$L_i \approx \frac{\lambda}{|J_{n-1}|}, \tag{C1}$$

where $\lambda > 0$ is the step length. For a piecewise constant Brownian process $\xi_i = \xi_{i-1} \pm \sqrt{\kappa\Delta_i}$ (the sign of $\sqrt{\kappa\Delta_i}$

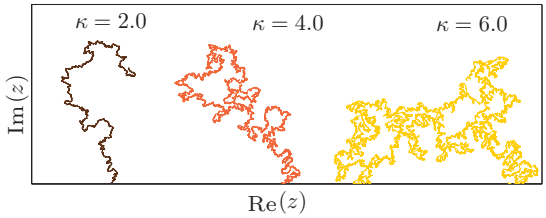

FIG. 3. (Color online) The N-SLE$_\kappa$ curves with length $N = 1 \times 10^4$, $\lambda = 0.001$, and $\kappa = 2.0$, 4.0, and 6.0 from left to right.

is chosen randomly according to the uniform probability distribution), the above approximation yields

$$\Delta_i = \frac{\lambda}{2\sqrt{\kappa}|G''_{i-1}(\xi_{i-1})|}. \tag{C2}$$

Note that computing points along the N-SLE$_\kappa$ curve requires this adaptive choice of Δ_i, and that the total time with these nonuniform time steps will be equal to $t_i = \sum_{n=1}^{i} \Delta_i$. In this procedure the distances between two sequential points $l_i \approx \lambda$ approximately remain constant.

In our study we followed one straightforward motivation for computing the Jacobian. If one considers $h_i(z) = f_i(z + \xi_i) - \xi_{i-1}$, the conformal map maps the upper half-plane onto the upper half-plane plus a slit. The length of this slit equals $2\sqrt{\Delta_i}$ and the position on the real line equals $\delta_i = \xi_i - \xi_{i-1}$. Following a simpler strategy one can decompose the incremental map $h_i(z)$ to $h_i(z) = T_{\delta_i} \circ \phi_i^{\mathbb{H}}$, where $\phi_i^{\mathbb{H}} = \sqrt{z^2 - 4\Delta_i}$ is the slit map and $T_{\delta_i}(z) = z + \delta_i$ is a translation map by the real value δ_i. The ith points of the SLE or N-SLE curve computed from $\gamma(t_i) = g_n(0)$, where

$$g_n(z) = T_{\delta_1} \circ \phi_1^{\mathbb{H}} \circ T_{\delta_2} \circ \phi_2^{\mathbb{H}} \circ \cdots \circ T_{\delta_i} \circ \phi_i^{\mathbb{H}}(z). \tag{C3}$$

We now consider a new format of Eq. (C2) as

$$\Delta_i = \frac{\lambda}{2\sqrt{\kappa}\,|g''_{i-1}(0)|}, \tag{C4}$$

where

$$g''_i(0) = |\phi''_n(0)| \prod_{j=0}^{n-2} |\phi'_{n-1-j}(\Gamma_j)|\,. \tag{C5}$$

In the above equation, Γ_j is defined as

$$\Gamma_j = T_{\delta_{n-j}} \circ \phi_{n-j}^{\mathbb{H}} \circ T_{\delta_{n-j+1}} \circ \phi_{n-j+1}^{\mathbb{H}} \circ \cdots \circ T_{\delta_n} \circ \phi_n^{\mathbb{H}}(0). \tag{C6}$$

Following [39] the proposed method of approximating sample paths of N-SLE$_\kappa$ consists of six steps: (1) Set the constants λ, κ, and N. (2) Set $n = 1$ and $\Delta_1 = 1$. (3) Compute $\sqrt{\kappa\,\Delta_n}$ according to steps 1 and 2 with a random sign ($\pm$) with equal probability. (4) Calculate $\gamma(t_n) = g_n(0)$ using the iteration map as shown in Eq. (C3). (5) Compute Δ_{n+1} using Eqs. (C2), (C5), and (C6). (6) If $n < N$ increase n by 1 and repeat steps 3 to 6. The typical curves of the N-SLE$_\kappa$ for $\kappa = 2$, 4, and 6 are presented in Fig. 3.

[1] R. Metzler and J. Klafter, J. Phys. A: Math. Gen. **37**, R161 (2004).

[2] B. Avraham and S. Havlin, *Diffusion and Reactions in Fractals and Disordered Systems* (Cambridge University Press, Cambridge, United Kingdom, 2000).

[3] B. Berkowitz and H. Scher, Phys. Rev. Lett. **79**, 4038 (1997).

[4] H. Scher and M. Lax, Phys. Rev. B **7**, 4491 (1973).

[5] T. H. Solomon, Eric R. Weeks, and Harry L. Swinney, Phys. Rev. Lett. **71**, 3975 (1993).

[6] M. Wachsmuth, W. Waldeck, and J. Langowski, J. Mol. Biol. **298**, 677 (2000).

[7] E. Barkai, R. Metzler, and J. Klafter, Phys. Rev. E **61**, 132 (2000); R. Metzler and J. Klafter, Phys. Rep. **339**, 1 (2000).

[8] T. Koren, J. Klafter, and M. Magdziarz, Phys. Rev. E **76**, 031129 (2007); T. Koren, M. A. Lomholt, A. V. Chechkin, J. Klafter, and R. Metzler, Phys. Rev. Lett. **99**, 160602 (2007).

[9] B. J. West, M. Bologna, and P. Grigolini, *Physics of Fractal Operators* (Springer-Verlag, New York, 2003); R. S. Strichartz, *Differential Equation on Fractals* (Princeton University Press, Princeton, New Jersey, 2006).

[10] B. D. Hughes, *Random Walks and Random Environments*, Vol. 1 (Clarendon, Oxford, 1995).

[11] S. Redner, *A Guide to First-Passage Processes* (Cambridge University Press, Cambridge, United Kingdom, 2001).

[12] A. Lloyd and R. May, Science **292**, 1316 (2001); M. E. J. Newman, Phys. Rev. E **66**, 016128 (2002).

[13] J. Chuang, Y. Kantor, and M. Kardar, Phys. Rev. E **65**, 011802 (2001).

[14] R. M. Capocelli and L. M. Ricciardi, Biol. Cybern. **8**, 214 (1971).

[15] O. Benichou, M. Coppey, M. Moreau, P. H. Suet, and R. Voituriez, Phys. Rev. Lett. **94**, 198101 (2005).

[16] B. B. Mandelbrot, *The Fractal Geometry of Nature* (Freeman, New York, 1982).

[17] H. Liebowitz, *Fracture*, Vols. I–VII (Academic, New York, 1984).

[18] H. O. Peitgen, D. Saupe, Y. Fisher, M. McGuire, R. F. Voss, M. F. Barnsley, R. L. Devaney, and B. B. Mandelbrot, *The Science of Fractal Images* (Springer-Verlag, New York, 1988).

[19] B. Sapoval, A. Baldassarri, and A. Gabrielli, Phys. Rev. Lett. **93**, 098501 (2004).

[20] L. Niemeyer, L. Pietronero, and H. J. Wiesmann, Phys. Rev. Lett. **52**, 1033 (1984); G. Vecchi, D. Labate, and F. Canavero, J. Phys. D: Appl. Phys. **29** (1994).

[21] A. Zoia. Y. Kantor, and M. Kardar, Europhys. Lett. **80**, 40006 (2007).

[22] O. Schramm, Israel J. Math. **118**, 221 (2000).

[23] T. Kennedy, J. Statist. Phys. **128**, 1125 (2007).

[24] B. B. Mandelbrot and J. W. Van Ness, SIAM Rev. **10**, 422 (1968).

[25] Mingzhou Ding and Weiming Yang, Phys. Rev. E **52**, 207 (1995).

[26] J. Hinkel and R. Mahnke, Int. J. Theor. Phys. **46**, 1542 (2007).

[27] G. F. Lawler, O. Schramm, and W. Werner, Ann. Probab. **32**, 939 (2004).
[28] M. Bauer and D. Bernard, Phys. Rep. **432**, 115 (2006).
[29] W. Kager and B. Nienhuis, J. Stat. Phys. **115**, 1149 (2004).
[30] A. Celani, A. Mazzino, and M. Tizzi, J. Stat. Mech. P12011 (2009).
[31] I. M. Sokolov and J. Klafter, Chaos **15**, 026103 (2005).
[32] M. Magdziarz and K. Weron, Physica A **367**, 1 (2006).
[33] A. Janicki and A. Weron, *Simulation and Chaotic Behaviour of α-Stable Stochastic Processes* (Marcel Dekker, New York, 1994).
[34] G. Lawler, *Conformally Invariant Processes in the Plane*, Surveys and Monographs, Vol. 114 (American Mathematical Society, Providence, Rhode Island, 2005).
[35] J. Cardy, Ann. Phys. **318**, 81 (2005); V. Beffara, Ann. Probab. **36**, 1421 (2008); S. Rohde and O. Schramm, Ann. Math. **161**, 879 (2005).
[36] O. Schramm and S. Sheffield, Ann. Probab. **33**, 2127 (2005).
[37] S. Smirnov, C. R. Acad. Sci. Paris **333**, 239 (2001).
[38] T. Kennedy, e-print arXiv:math/0510604v1.
[39] M. Gherardi, J. Stat. Phys. **136**, 864 (2009); **140**, 1 (2010).
[40] G. F. Lawler, e-print arXiv:0712.3263v1; G. F. Lawler and S. Sheffield, e-print arXiv:0906.3804.
[41] P. Oikonomou, I. Rushkin, I. A. Gruzberg, and L. P. Kadanoff, J. Stat. Mech. P01019 (2008).
[42] E. Csaki, M. Csorgo, A. Foldes, and P. Revesz, J. Theoret. Prob. **9**, 745 (1996).